Clays and Clay Minerals, Vol. 45, No. 4, 564–579, 1997.

AN Fe-BERTHIERINE FROM A CRETACEOUS LATERITE: PART I. CHARACTERIZATION

THOMAS A. TOTH AND STEVEN J. FRITZ

Department of Earth and Atmospheric Sciences, Purdue University, West Lafayette, Indiana 47907

Abstract—An Fe-berthierine occurs in a buried laterite from the Late Cretaceous (Cenomanian) in southwestern Minnesota. It formed beneath a lignitic horizon in which reducing solutions percolated through a laterite comprising gibbsite, kaolinite and goethite. Morphologic differences suggest 2 separate conditions of Fe-berthierine formation. Early forms of Fe-berthierine include radial bladed or radial blocky crystallites coating pisoids, along with alteration of kaolinite at crystal boundaries. These morphologies formed in the vadose zone. Later forms precipitated under subaqueous conditions as macroscopic, pore-filling cement. The large size of the later-formed Fe-berthierines enabled microprobe characterization. This 1st reported occurrence of Mg-free berthierine has a structural formula close to an idealized Fe-berthierine: $Fe_2Al_2SiO_5(OH)_4$. Apart from their chemistry, the unique feature of the Minnesota Fe-berthierines is their formation in an exclusive nonmarine depositional environment. They formed *in situ* as part of a lateritic weathering profile developed on a broad, low relief peneplain. Physical evidence of formation under nonmarine conditions includes the presence of 1) scattered lignitic fragments; 2) concretions forming casts and molds of woody material; and 3) a nonmarine fossil (*Unio* sp. undet). Chemical evidence includes siderites collected from the berthierine-bearing horizon having stable isotope values indicating freshwater formation.

Key Words—Berthierine, Cretaceous Weathering, Kaolinite, Minnesota, Pisoid.

INTRODUCTION

Berthierine is an Fe-Al, 1:1-type layer silicate with a basal spacing of 7 Å, belonging to the serpentine group. Brindley's (1982) generalized formula for this mineral is $(R^{2+}_a R^{3+}_b \square_c)(Si_{2-x}Al_x)O_5(OH)_4$, where R^{2+} consists of Fe(II), Mg(II) and Mn(II); R^{3+} consists of Fe(III) and Al(III) in octahedral positions; and $\square$ represents possible vacant octahedral positions. Because Fe-rich chlorites have very weak 14-Å reflections on X-ray diffractograms, berthierine is difficult to resolve from chlorites. Thus, berthierine is frequently mistaken for chamosite, which is the 14-Å, 2:1-type layer silicate representing the Fe-rich chlorite end member. Moreover, the presence of kaolinite often masks the presence of berthierine due to the close proximity of (001) and (002) reflections of these 2 minerals. Although berthierine was identified prior to Brindley's (1982) paper, its recognition in sediments has been more frequent since Brindley's publication.

The 1st part of this 2-part study reports on the geologic setting, mineral association, morphology and chemistry of berthierine from a Late Cretaceous laterite in southwestern Minnesota. Its chemistry approaches that of an idealized Fe-berthierine ($Fe_2Al_2SiO_5[OH]_4$) which is essentially free of Mg based upon results of 91 microprobe analyses. (Hereafter, this Mg-free berthierine from Minnesota is referred to simply as Fe-berthierine). This Fe-berthierine forms unusually large, macroscopic pore-filling cement lining voids between pisoids that developed on a laterite. Other forms include radial bladed and blocky pore coatings and as replacement of kaolinite along pseudohexagonal crystal boundaries. The composition of this 4-oxide component berthierine, in conjunction with chemistries of gibbsite, kaolinite, goethite and siderite with which it is in equilibrium, allows a portrayal of the physicochemical conditions responsible for this assemblage. These calculations are presented in the ensuing paper along with results of modeling detailing the conditions under which Fe-berthierine will or will not form.

Past Reportings of Berthierine

Table 1 lists mineral associations, geologic settings, forms and localities for berthierine as reported by past workers. Berthierine usually comes from marine rocks or from sediments influenced by marine waters during early diagenesis. Van Houten and Purucker (1984) described occurrences of oolitic ironstone (many containing berthierine) throughout geologic time and attributed their formation to low-energy environments on inner-embayed shelves in tropical to subtropical regions. They, along with Hallam and Bradshaw (1979), recognized the importance of ironstones as indicators of condensed sections forming sequence or parasequence boundaries in marine rocks.

Forms in which berthierine have commonly been described included alternating sheaths and coatings of pisoids and ooids (Bhattacharyya 1983, 1989), replacement of bioclastic material (Kearsley 1989), pellets associated with goethite in the Niger Delta (Porrenga 1966, 1967) or late-formed cement (Lu et al. 1994). Siehl and Thein (1989) describe the source area of Minette-type ironstones as a low relief, iron hy-

droxide and kaolinite-rich capped peneplain, with a lateritic source for the ferruginous pisoids and ooids. Repeated reworking of these hydromorphic soils and mud flats preconcentrated ferruginous microconcretions and duricrust fragments which were subsequently washed into the sea and winnowed by wave agitation and accumulated as marine ironstones. No distinct terrestrial facies is recognized in the Minette ironstones, nor is there any sign of fresh-water influences. Siehl and Thein (1989) attribute berthierine formation to diagenetically altered aluminous goethite; yet they do not comment on the source of silica needed to form berthierine.

Few studies describe berthierine from purely continental settings. Taylor (1990) investigated the Early Cretaceous Wealden sediments of southeast England and described an intraformational conglomerate containing pisoids and pseudo-ooids with a quartz–siderite–berthierine mineral assemblage deposited in a fresh-to-brackish-water mudplain. The pisoids and ooids were derived from Fe-rich soils that were eroded and deposited in the basal part of a scour-filled conglomerate and diagenetically transformed after burial. Meyer (1976) describes Wealden sediments from the Paris basin as being deposited on a very mature floodplain with *in situ* weathering by soil processes with a warm climate and repeated wetting and drying leading to a quartz–kaolinite–goethite–illite–chlorite mineral assemblage. Although he does not observe any berthierine, the etching shown on quartz grains in the soil horizon provided evidence of intense leaching. Iijama and Matsumoto (1982) describe berthierine from fresh-water coal swamps based on the close association between fossil plant leaves and coal seams with no marine fossils. This nonmarine berthierine occurs in a cryptocrystalline mixture with kaolinite as a matrix in siderite concretions. Authigenic siderite was always observed in association with berthierine, except where it is completely replaced by berthierine and quartz. Nikitina and Zvyagin (1972) observed bauxites reworked under swampy-lagoonal conditions with epigenetic minerals superimposed on the bauxitic sediments under reducing conditions containing a 7-Å chlorite (possibly berthierine?) that formed at the expense of kaolinite. The Fe-silicate phase (either berthierine or chamosite) also had a significant Mg component.

Modern authigenic berthierine occurs in the form of pods such as fecal pellets or test fillings (Harder 1989) and as envelopes around sand grains (Rohrlich et al. 1969). Morphologies from sedimentary rocks include pisoids with no concentric ring structure (Schellmann 1966) and oolites (Velde 1989), both as aggregates and as alternating cortical sheaths (Bhattacharyya 1983) and as ultrafine mineral assemblages (Hughes 1989). Kearsley (1989) describes several forms of berthierine occurring in Fe-rich ooids based on the dominant mineral associations. These multiple morphologies are characterized by small grain size, in the range of 1–10 μm, with the exception of replacement of bioclastic grains.

The above references are not meant to constitute an exhaustive review. But, in conjunction with Table 1, the reader should conclude that past reportings of berthierine are: 1) mainly marine; 2) always associated with reducing conditions; 3) associated with siderite; 4) associated with pisoids or ooids; and 5) deposited during times of reduced sediment influx.

METHODOLOGY

A 13-m section of unconsolidated kaolinitic sands, silts and muds located along Purgatory Creek in Renville County, Minnesota, is capped by a 6-m-thick laterite characterized by an indurated, pisolitic texture (Figure 1). Of that 13-m section, the lower 5 m are presently covered and the upper 4 m inaccessible. An interval of 0.5 m was used to collect samples from the remaining 4 m.

Optical microscopy, scanning electron microscopy (SEM), back scattering imagery and elemental X-ray analyses characterized the morphology and texture of the Fe-berthierine. An automated 4 spectrometer CAMECA SX-50, operated at 20 nA/15 keV with a 10 μm-diameter beam size, provided geochemical data of the macroscopic berthierine. An attempt to determine the Fe(III)/Fe(II) ratio by the wet chemical method of Fritz and Popp (1985) was unsuccessful due to paucity of impurity-free, hand-picked grains. With the low ferric component of published chemistries, and the inability of the microprobe to distinguish valence states, all Fe values are reported as total Fe as FeO. This has become common procedure for investigations of berthierine and chlorites using electron microprobe (EMP) analyses (Iijama and Matsumoto 1982; Maynard 1986; Taylor 1990). Distinctions between berthierine and Fe-stained kaolinite utilized elemental X-ray analyses by scanning at 2-μm steps for Si, Al, Fe and Mg. Back scattering imagery increased the resolution, showing the various morphologies of the Fe-berthierine. SEM analyses were also used for characterization and showing intergranular relationships.

The aforementioned analytical methods provided geochemical and morphological data of the presence of an Fe silicate. Conclusive confirmation of berthierine utilized both powder and single-crystal X-ray diffraction (XRD) methods. Mineral assemblages were confirmed from powder diffraction patterns from bulk samples of both pisolitic material and its matrix, along with hand-picked samples containing abundant macroscopic berthierine. A scanning speed of 0.2 °2θ/min was used with an accelerating voltage of 45 keV and a current of 25 mA. Single-crystal X-ray analysis was kindly provided by S. Guggenheim. Stable isotopic values for ^{13}C and ^{18}O were determined at the Envi-

Table 1. Reported berthierine occurrences listing their location, geologic setting, forms, mineral associations and references.

Number	Location	Geologic setting	Forms†
1–3	Belgorod District—Kursk (USSR)	bauxite	pis-cem
4	Wabana, Newfoundland (Canada)	hematitic ironstone	oo
5–6, 11	Voronezh Anticline—Kursk (USSR)	bauxite	pis-crypt
7	Ayrshire (Scotland)	lateritic claystone	crypt
8	Weald—Sussex (England)	brackish water mudplain	pis
9	Stanion Lane Pit—Corby (England)	sand ironstone	oo
10	Pegnitz (Germany)		
12	Gunflint Range, Minnesota (USA)	banded iron formation	
13	Sainte-Barble (France)	minette ironstones	oo
14	Kank—Kutna Hora (Czech)		
15	Chamosentze (Switz)	minette ironstones	oo
16	Windgalle (Switz)	minette ironstones	oo
17	Schmiedefeld (Germany)	minette ironstones	oo
18	Gledic (Yugoslavia)	chamositic bed	
19	Isle of Raasay (Scotland)		oo
20	Frodingham (England)		
21	Loch Etive (Scotland)	brackish—cold water	pel
22	Canadian Arctic (Canada)	modern—soil	
23–24	Niger Delta (Niger)	modern—delta	pel
25	Algeria (Algeria)		
26	Arakawa Mine—Akita (Japan)		
27	Amazon Mouth (Brazil)	modern—delta	
28–31	Central Appalachians, Virginia (USA)	hematitic ironstone	coat
32–34	Hiramatsu—Utatsu District (Japan)	coal measures	crypt
35	Algeria (Algeria)	breccia—marine	pel
36–37	Weald—Sussex (England)	brackish water mudplain	pis
38	Frodingham—Yorkshire (England)		oo
39	Northhampton—Corby (England)	sand ironstone	oo
40	Mines a Poix (France)	minette ironstones	oo
41	Wabana, Newfoundland (Canada)	hematitic ironstone	oo
42	Ardnish Skye (Scotland)	lateritic claystone	oo
43	Cleveland—Yorkshire (England)		oo
44	Langrial (Pakistan)		oo
45	Rockwood, Tennessee (USA)	hematitic ironstone	oo
46	Raasay Skye (Scotland)		oo
47	Clinton—Little Falls, New York (USA)	hematitic ironstone	oo
48	Clinton—Oneida, New York (USA)	hematitic ironstone	oo
49–50	Cenomanian, Minnesota (USA)	laterite	cem-coat

† Form labels include: oo = ooids, pis = pisoids, coat = coatings, pel = pellets, cem = cement, crypt = cryptocrystalline, bio = bioclast replacement, rep = replacement.

‡ Mineral labels include: kao = kaolinite, gib = gibbsite, goe = goethite, sid = siderite, hem = hematite, pyr = pyrite, cha = chamosite, qtz = quartz, boe = boehmite, gla = glauconite, chl = chlorite, gyp = gypsum, fel = feldspar, hbl = hornblende, mica = micaceous minerals.

§ Breaks in table indicate either the author did not include that data in his or her publication, or that the reference was not obtainable.

ronmental Isotope Lab of the University of Waterloo, Ontario, for siderites obtained from both berthierine-bearing and non-berthierine-bearing pisolitic horizons found at the top of the kaolinitic sediments. Analyses for ^{13}C and ^{18}O are reported relative to PDB and SMOW, respectively.

RESULTS

Geologic Setting

Basal Cretaceous deposits found in outcrops along the Minnesota River valley in southwestern Minnesota consist of unconsolidated kaolinitic sand, silt and clay (Sloan 1964; Parham 1970; Toth 1991; Setterholm 1994). These sediments were deposited in fluvial systems that incised into a Late Cretaceous weathering profile (Figures 2a–b) developed on the 3.6-Ga Morton Gneiss—a lithology of some renown due to its use by Goldich (1938) as the basis for his mineral-stability series. They are Early Cenomanian age and represent sediments associated with transgression of the Greenhorn cyclothem of the Western Interior Seaway (Setterholm 1994; Toth 1996). All sediments were derived locally from the saprolite and consist of quartz and kaolinite, with minor altered feldspar, and trace amounts of ilmenite, sphene, apatite, zircon and magnetite. These deposits, overlying the weathered saprolite and overlain by organic-rich, kaolinitic silt and clay, are correlative with the Nishnabotna Member of the Dakota Formation (Toth 1996), and can be subdivided into 2 separate parts: a

Table 1. Extended.

Mineral associations‡	References
hem-kao-boe	Klekl 1979
hem-cha-sid	Brindley 1951
qtz-hem-goe-kao	Yershova et al. 1976
sid-kao	Brindley 1951
§	Thurrell et al. 1970
sid-lim-qtz-gyp	Brindley and Youell 1953
	Halbach 1970
	Floran and Papike 1975
	Deudon 1955
	Novak et al. 1957
	Deverin 1945
	Deverin 1945
	Jung, by Engelhardt 1942
	Protich 1955
goe	MacGregor, Lee, and Wilson 1920
goe	Hallimond et al. 1939
qtz-chl-fel-hbl-mica	Rohrlich et al. 1969
	Kodama and Foscolos 1981
qtz-gla-goe	Porrenga 1966
	Porrenga 1966
	Sudo 1943
qtz	Rude and Aller 1989
hem-qtz	Lu et al. 1994
kao-sid-goe-chm	Iijama and Matsumoto 1982
chl-gla-cal-alb	Velde et al. 1974
qtz-sid-hem	Taylor 1990
boe	Maynard 1986
sid-lim-qtz-gyp	Maynard 1986
goe-hem	Maynard 1986
hem-cha-sid	Maynard 1986
	Maynard 1986
sid	Maynard 1986
hem-cha	Maynard 1986
hem-cha-pyr	Maynard 1986
goe	Maynard 1986
cha	Maynard 1986
hem	Maynard 1986
kao-gib-goe-sid	This study

lower arenaceous zone and an upper argillaceous zone (Figure 3).

The lowermost part of the arenaceous zone is conglomeratic at the base, with angular cobbles of milky-white vein quartz and oblate kaolinitic intraclasts within a kaolinitic matrix. The conglomerate grades into interlayered fine-grained sand-to-silt. The matrix coating the grains is mostly cryptocrystalline kaolinite with scattered micaceous flakes of kaolinite, indicating that biotite from the gneiss was completely altered by intense chemical weathering. The sediments were deposited in low-sinuous, low-gradient streams. Regional mapping by Toth (1996) indicates that the conglomeratic kaolin was deposited in the main, fluvial channel, followed by an upward change into crevasse-splay channel sands and natural levee deposits. The fine-clay intraclasts were deposited in adjacent floodplains as overbank fines and reworked by flooding (Figure 2c). Extended periods of stream stability led to the incipient formation of pisoids, representing minor hiatus surfaces that record periods of nondeposition or minor regressions of the Seaway.

Stream gradients decreased with transgression of the Western Interior Sea. This resulted in more sluggish streams and deposition of alternating finer-grained silts and muds. The upper, argillaceous zone is characterized by silt and clay with thin, fine-sand layers and organic-rich lag deposits. Capping these deposits is a laterite that forms an areally extensive pisolitic horizon (Parham 1970), ranging in thickness from 1–6 m, which represented the longest duration of stream stability. (Other pisolitic horizons lower in the section contain centimeter-thin, laterally extensive incipient pisoids, representing stream stability of much shorter duration). This laterite consists of indurated kaolinitic, goethitic and gibbsitic pisoids that increase in quantity upwards from a few scattered pisoids within silt and clay to a completely pisolitic horizon that obliterates any primary sedimentary structures or bedding. Occurrences of Fe-berthierine are from the laterite exposed along Purgatory Creek. No evidence of reworking of pisolitic material in the argillaceous zone was observed. Pisolitic zones are confined to silt and mud zones whereas minor amounts of pisoids are present in sandy zones. No channels are observed at the base of pisolitic horizons which would indicate reworking or transported nature of pisolitic material similar to the formation of the Wealden deposits described by Taylor (1990).

Disconformably overlying the laterite are organic-rich silt and clay with thin, discontinuous lignites and bentonites. These deposits are correlative with sediments of similar lithology from Iowa which Witzke and Ludvigson (1994) interpreted as being deposited in backwater swamps in interchannel wetlands (Figure 2d). Preservation of lignitic material represented a climatic change from one where organic material is quickly recycled (except for woody tissue) to one where it is preserved. The only example of reworked pisolites occurs about 10 km west of the Purgatory Creek location at a commercial clay pit where the lower 0.5 m of organic-rich mud contains a 0.2-m-thick layer of transported pisoids reflecting localized reworking. Parham (1970) and Setterholm (1994) describe marine sediments overlying the organic-rich, nonmarine deposits and Bolin (1956) collected samples of marine *foraminifera* and ostracods from the Redwood Falls area, 20 km west of Purgatory Creek. It is not known whether the samples were collected from *in situ* or glacially reworked sediments. Figures 2e–f show the gradual transgression and later scouring and deposition associated with Pleistocene glaciation.

Mineral Associations

XRD showed the presence of gibbsite, kaolinite, berthierine, siderite and goethite as major phases

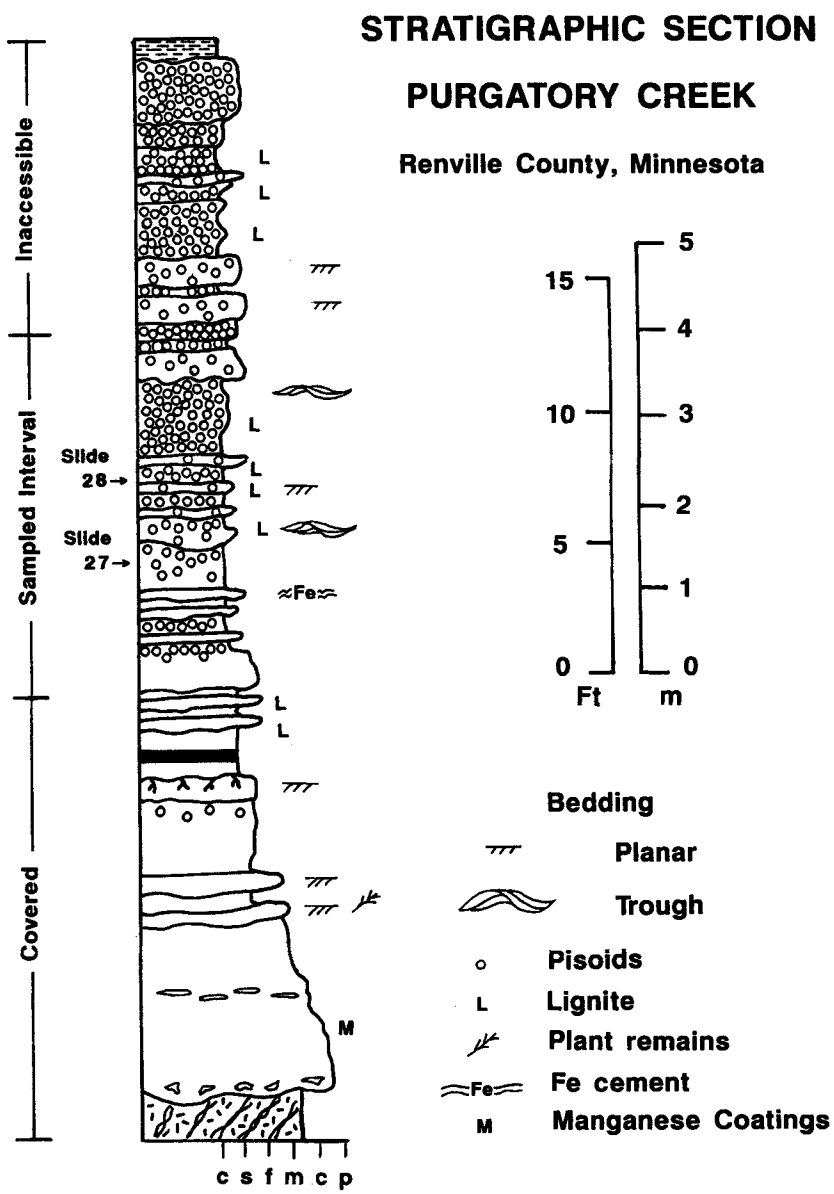

Figure 1. Stratigraphic column for the Fe-berthierine-bearing rocks from Purgatory Creek. Pisoid abundance reflected in density of (○) symbols. Also shown is the position of samples taken from which chemistry of berthierine is reported. The upper 0.25 m of the section consists of organic-rich silts and clays.

along with minor amounts of boehmite, nordstrandite, and vivianite (Figure 4). To delineate kaolinite from berthierine, only samples with macroscopic berthierine were chosen for XRD analysis (Figure 5). Using a shorter step interval and longer count time, berthierine (001) and (002 peaks) were differentiated from those of kaolinite (Figure 5). Powder patterns of crushed crystals indicated that they were composed of 2 different polytypes, a trigonal (*1T*) and a monoclinic (*1M*) form, with trigonal forming the dominant polytype. Single-crystal methods showed a complete random stacking (S. Guggenheim, personal communication).

An unusual relationship exists between the results of the single- and crushed-crystal XRD methods and the high Al content for this Fe-berthierine. Brindley (1982) and Bailey (1988) observed that berthierines with high Al_2O_3 appear more commonly in the *1M* polytype, and that the *1T* polytype is more common in samples with low Al_2O_3 and high SiO_2 contents. The Minnesota Fe-berthierine is predominately the *1T* polytype, yet its chemistry agrees with that found with

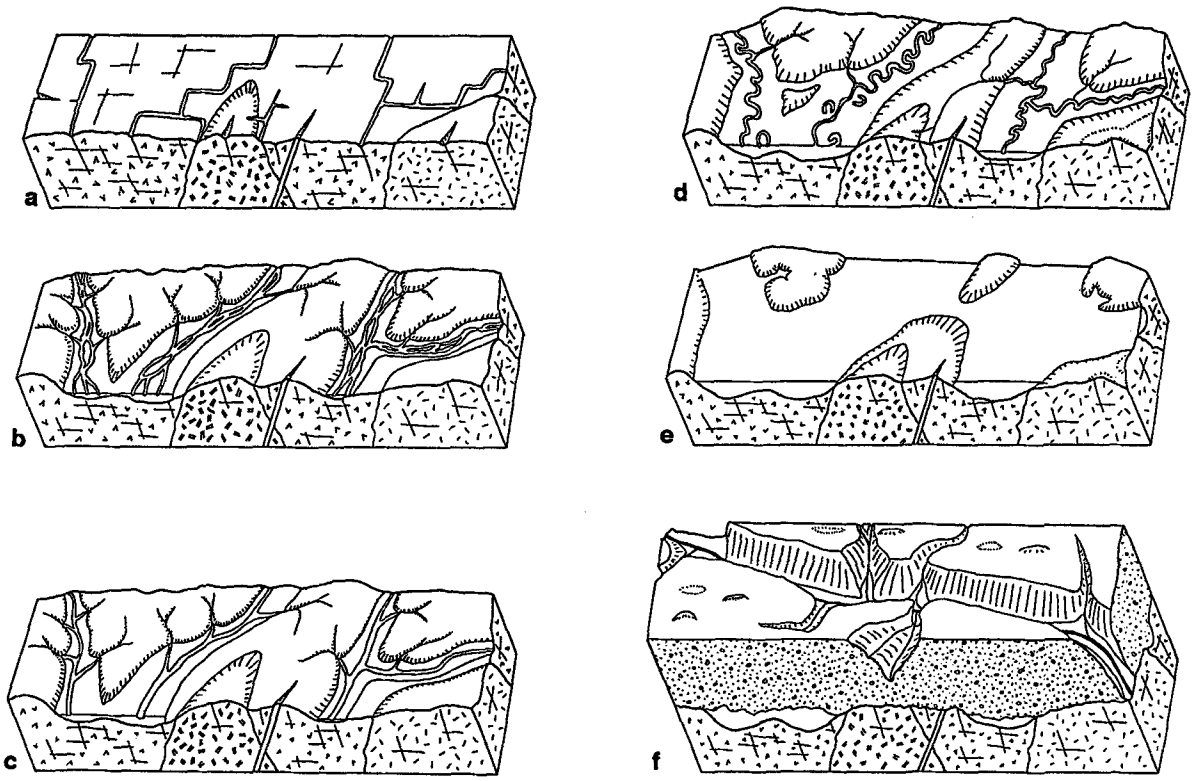

Figure 2. Paleogeographic reconstruction of the Minnesota River Valley reflecting Late Cretaceous weathering and transgression of the Western Interior Sea. a) Late Albian—initiation of saprolite formation with drainage confined to structurally resistant joints and fractures. b) Late Albian–Early Cenomanian regression—led to development of braided streams confined to incised valleys. c) Early Cenomanian stillstand—resulted in graded streams and development of pisolitic horizons. Several of these episodes are recorded, with the longest period of pisoid development occurring at the top of the section. d) Early Cenomanian onset of transgression—lowering of stream gradient caused change in fluvial environment from graded to meander belt system. Resulted in deposition of lignitic shales overlying laterite. e) Late Cenomanian–Early Turonian transgression—inundation of study area during maximum flooding of Greenhorn Transgression. f) Modern—reflecting deposition and erosion of glacial drift.

the *1M* polytype. This is probably a function of the random ordering observed from single crystals and will not be resolved until a more ordered form is analyzed.

The arenaceous and argillaceous zones give clues relative to the paragenesis of Fe-berthierine. Sediments from the arenaceous zone have a simple mineral assemblage consisting of kaolinite and quartz with some horizons characterized by goethitic staining, others by sideritic concretions (Figure 3). Trace amounts of ilmenite, sphene, rutile, apatite and zircon reflect sediment derivation from the Morton Gneiss and related granitic phases. The quartz sand and silt is commonly coated with an amorphous Fe stain. This Fe-coated quartz is found throughout the section. Incipient pisoids in the arenaceous zone are composed of kaolinite that is outlined by either goethite, kaolinite or an amorphous Fe coating.

Sediments from the argillaceous zone contain the same major minerals as the underlying arenaceous zone, but with kaolinite content much greater than quartz. The laterite, however, has a more complex mineral assemblage (Figure 3). Kaolinite, gibbsite and goethite form the major minerals present. Quartz is a minor component. Berthierine occurs only in the laterite in minor-to-trace amounts, and always in association with kaolinite. Berthierine is present only in horizons showing evidence of reducing conditions. These horizons are characterized by a green-to-black colored matrix and the presence of lignite. Horizons not containing berthierine have a yellow-to-red matrix indicative of oxidative conditions. Siderite occurs in minor-to-trace amounts, either in association with goethite, or as neoformed crystals associated with both a kaolinitic porcelaneous cement and detrital cryptocrystalline masses of kaolinite. Both the arenaceous and argillaceous zones have resistate assemblages indicating extreme weathering conditions in which all alkaline elements have been leached. Partial to complete dissolution of quartz is evidenced by Fe-stained coatings forming the outer part of molds of voids,

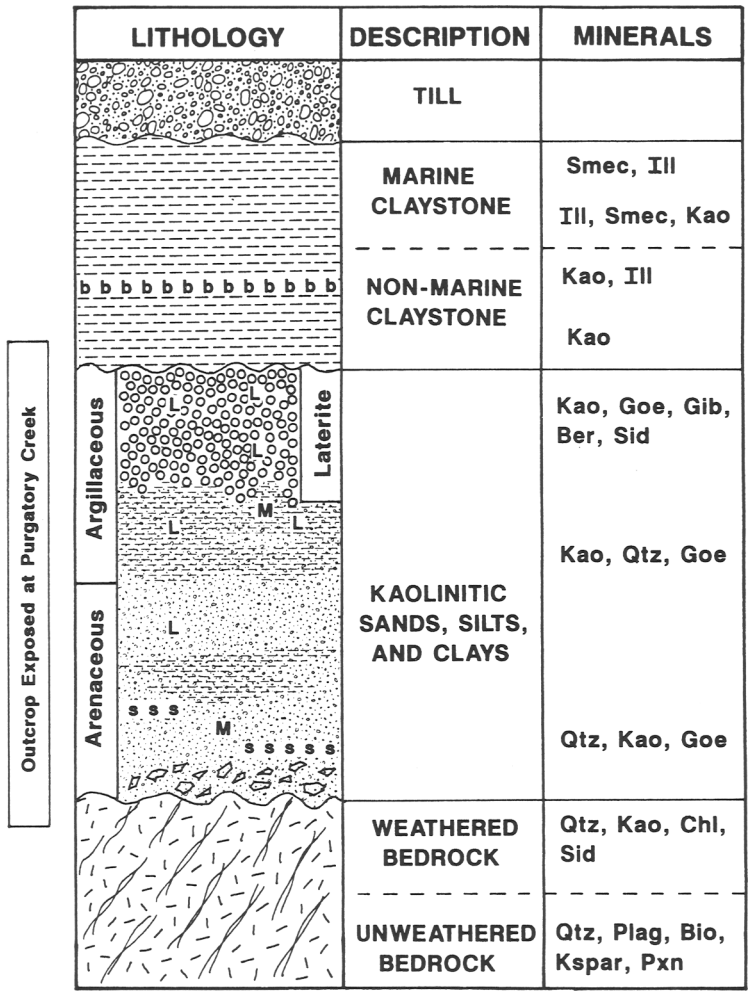

Figure 3. Composite stratigraphic section for Upper Cretaceous sediments of the Minnesota River Valley showing associated major minerals present in distinct lithologic units. All units below Till are Cretaceous. Differential erosion resulted in Till resting unconformably over all Cretaceous units and bedrock. Symbols include: b = bentonite, M = manganese coatings, s = siderite concretions/Fe-staining, L = lignite cement.

some containing weathered quartz grains leached to much smaller sizes than the void space.

Organic matter in the form of lignitic fragments is scattered throughout the upper part of the argillaceous zone. The presence of siderite and berthierine in the laterite indicates a period where localized or solution-front reducing conditions were favorable. This is supported by their occurrence only in that part of the laterite containing the green-to-black colored matrix. These ferrous-bearing minerals could not have formed without the presence of organic matter, indicating the relationship between organic matter and early diagenesis (Curtis 1995).

The 2 major minerals (kaolinite and quartz) differ slightly in their forms found in the 2 zones. Quartz in the arenaceous zone ranges in size from fine sand and silt near the top to angular cobbles at the base, and from silt to fine sand in the argillaceous zone. Kaolinite from the arenaceous zone occurs as cryptocrystalline matrix, vermiform booklets and large (millimeter-size) equant grains resulting from feldspar alteration or micaceous grains resulting from mica alteration. The argillaceous kaolinite is also cryptocrystalline, but with inclusions of amorphous Fe stains, and smaller, authigenic vermiform booklets. No large grains are present, reflecting the fine-grain-sized sediment associated with overbank fines and crevasse-splay deposits. A gray, amorphous opaline-looking, porcelaneous cement found between pisoids is also kaolinite. This gray cement contains minute red particles of goethite or large (1 mm) saucer-shaped siderite.

Gibbsite is confined to the pisolitic horizon and formed at the expense of kaolinite with subsequent silica leaching (Figure 6). It occurs as a brown matrix or as pisoids that commonly are also kaolinitic. Gibbsite is present only as altered grains with no evidence

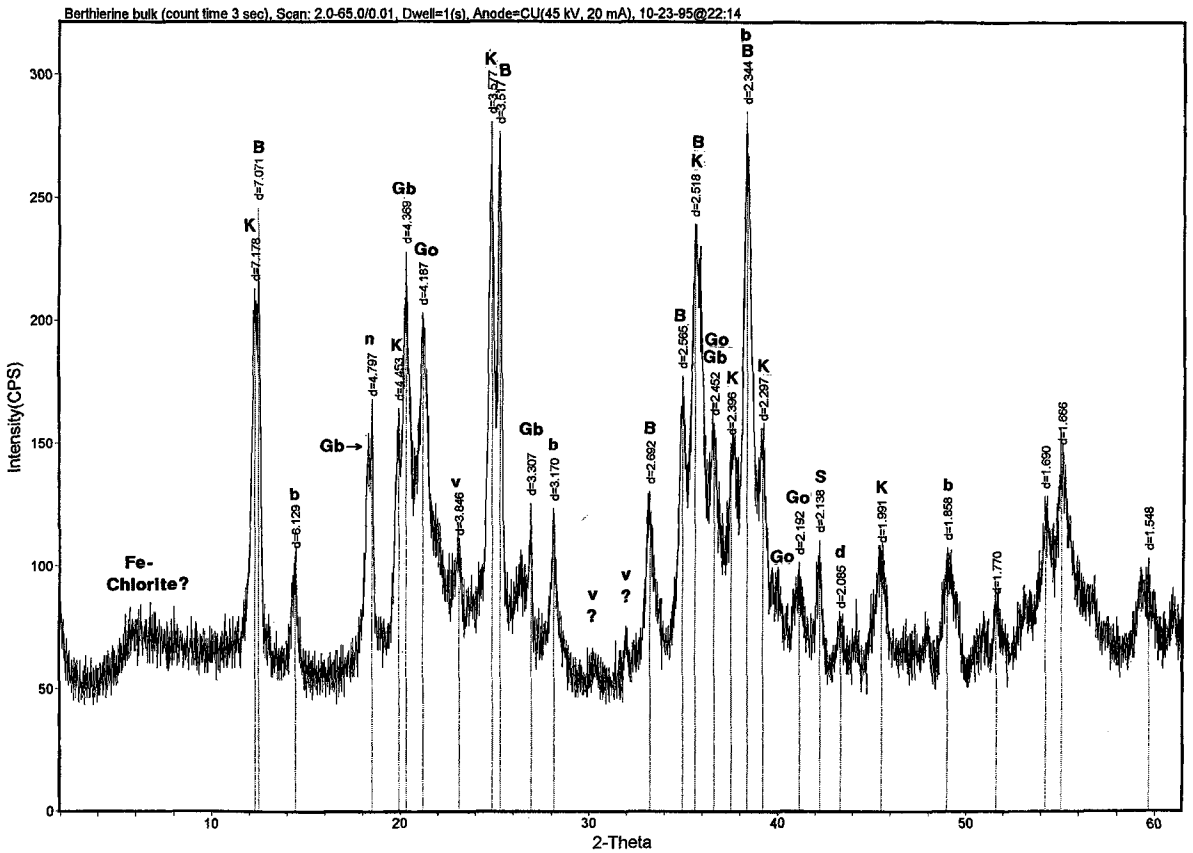

Figure 4. Random powder diffractogram of material from which Slide 27 was collected. Peak labels include: K = kaolinite, B = Fe-berthierine, Gb = gibbsite, Go = goethite, S = siderite, d = diaspore, n = nordstrandite, v = vivianite and b = boehmite.

of authigenic grains or cement. Goethite occurs as brown, red or yellow coatings or stains on pisoids, as irregular-brown masses that are intermixed with kaolinite and as coatings on quartz grains. Trace amounts of crandallite occur in association with berthierine and represent alteration of apatite.

The overlying nonmarine and marine silts and muds show a systematic change in clay mineralogy reflecting the transgression of the advancing sea and shoreward movement of marine facies (Figure 2). The nonmarine sediments are predominately kaolinite, but show a gradational change to an illite–kaolinite assemblage followed by an illite–smectite assemblage (Parham 1970). Only the basal part of the nonmarine, organic-rich silts and clays (Figure 1) is preserved above the laterite at Purgatory Creek (the uppermost lithology on Figure 1). Pleistocene glacial activity removed the upper nonmarine sediments.

Morphology

The Fe-berthierine from Minnesota has 4 distinct morphologies. Earlier-formed berthierine occurs as fine-grained radial blades coating the outer rims of pisoids (Figure 7). This radial, grain-coating Fe-berthierine is found as tufts of crystallites, or as blocky crystallites with the longest dimension oriented normal to the coated grain. There is an abrupt termination of the crystallites at the base, supporting formation of the crystallites as a precipitate from solution, not alteration of the outer part of the enclosed grain. Photomicrographs of back-scattered electron images show a similar radial coating of pisoids, but also with the blocky habit (Figure 8). Figure 9 shows the transformation of kaolinite to berthierine with the berthierine occurring within the pisolitic kaolinite. Berthierine found in pseudohexagonal patterns (intersecting lines at 60 to 120°) suggests that alteration of kaolinite occurred along outer edges of vermicular grains that are commonly found in the kaolinitic sediments. These 3 forms (radial bladed, radial blocky and cleavage alteration) show the intergranular relationship between berthierine and associated pisoids that formed in hybrid open-system dissolution of groundwater.

The 4th morphology is the most significant. Here, the Fe-berthierine occurs as pore-filling cement, which is macroscopic in hand samples. Its large grain size

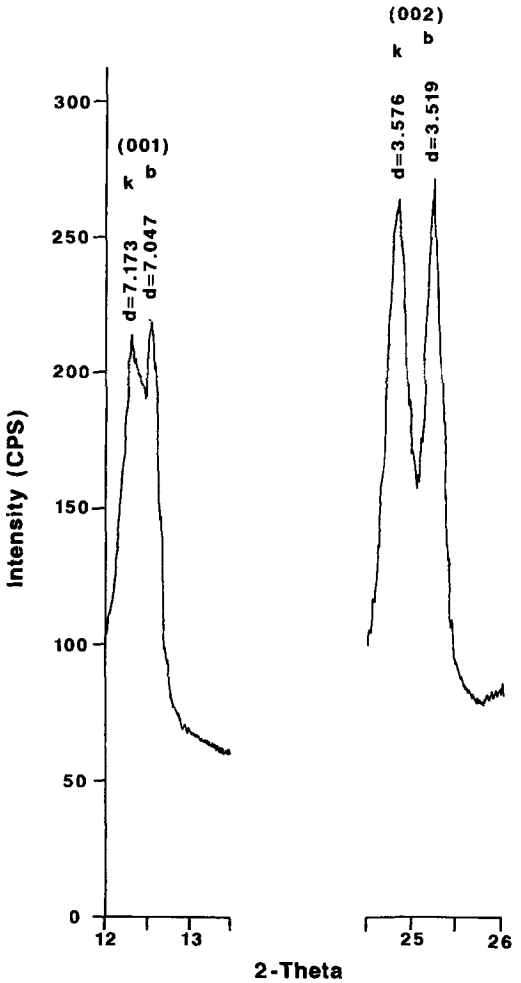

Figure 5. Portions of random powder diffractogram showing delineation of kaolinite and Fe-berthierine (001) and (002) peaks. A count time of 20 s was used.

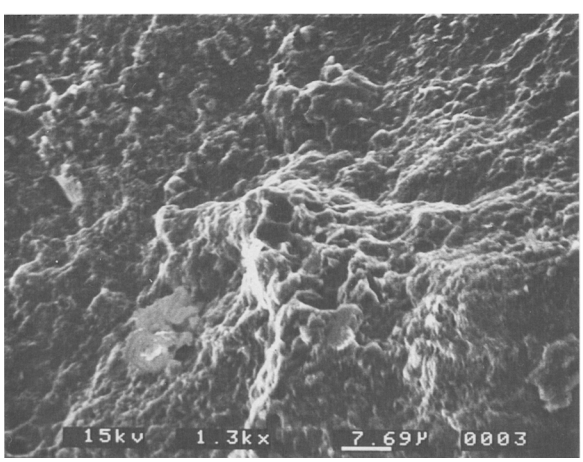

Figure 6. Scanning electron photomicrograph of detrital kaolinite. Large grain in center is kaolinite with alteration of outer edges to gibbsite.

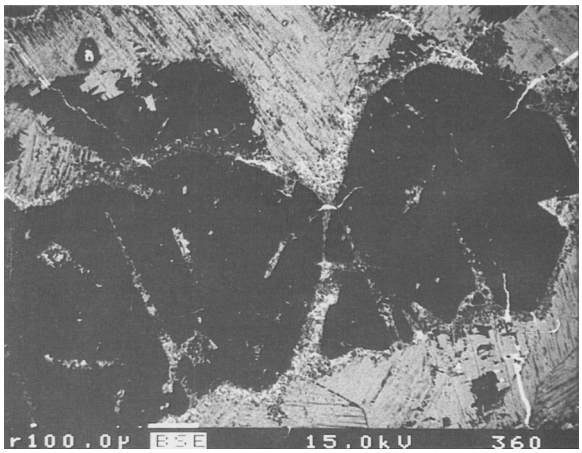

Figure 7. Back-scattered electron photomicrograph of early-formed, bladed Fe-berthierine (gray) forming a coating around kaolinitic pisoids (blacks). Lighter matrix is late-forming, macroscopic Fe-berthierine. Electron microprobe analyses of Fe-berthierine was obtained from this form.

(relative to the other 3 morphologies) indicates that it formed more slowly under subaqueous conditions. These occur as pale- to dark-green, micaceous grains with well-developed basal cleavage which can be separated easily from the laterite. These forms have a maximum dimension of 300–700 µm, and in places form the bulk mineralogy of the rock (Figure 10). The large size of these grains allowed for reliable geochemistry from microprobe analysis in which sufficient sample is present with no impurities.

Chemistry

Our microprobe results of the Fe-berthierine provide evidence of the 1st reported occurrence of an Fe-berthierine. The compositions of this berthierine, sampled from 2 horizons, are listed below:

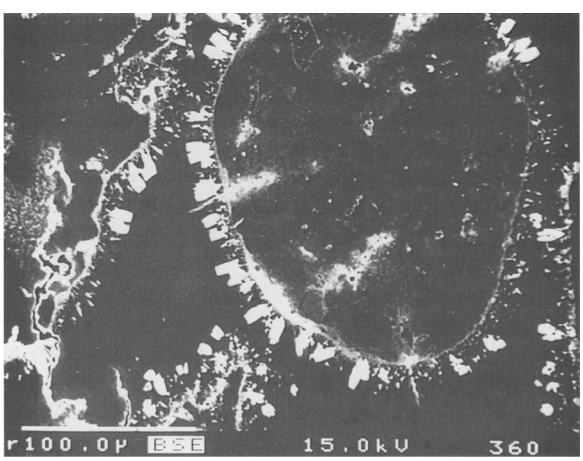

Figure 8. Back-scattered electron photomicrograph of early-formed, blocky Fe-berthierine (white) coating kaolinitic pisoid (gray). Dark gray matrix is also kaolinite.

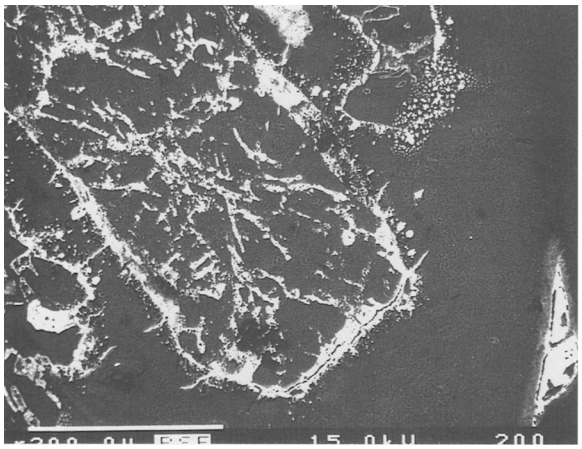

Figure 9. Back-scattered electron photomicrograph of early-formed, bladed and blocky Fe-berthierine (white) coating kaolinitic pisoid (gray). Alteration of kaolinite to Fe-berthierine within pisoid occurred along pseudohexagonal crystal boundaries.

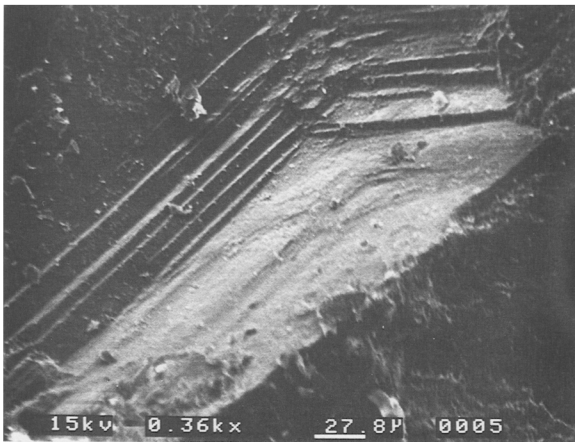

Figure 10. Scanning electron photomicrograph of late-forming, macroscopic Fe-berthierine.

Slide 27 $(Mg_{0.007}Fe^{II}_{2.084}Al_{0.899}\square_{0.010})(Al_{0.884}Si_{1.116}O_5)(OH)_4$

Slide 28 $(Mg_{0.006}Fe^{II}_{2.126}Al_{0.886})(Al_{0.920}Si_{1.080}O_5)(OH)_4$

Slide 27 represents a composite of 52 microprobe analyses from 5 transects, whereas 39 analyses from 3 transects were used for Slide 28. All analyses were taken from centimeter-sized, pore-filling cement. The sample from which Slide 28 was prepared was collected 2 m above the sample used for Slide 27 (Figure 1). Relative to previously published analyses, these compositions differ in the following ways: 1) They have the lowest Mg content of any published berthierine analyses. The maximum MgO wt% for the probed Fe-berthierines is 0.12%, with an average of 0.08%—equivalent to 0.007 mol in octahedral coordination. Typical Mg(II) molar content of previously reported compositions is 0.30, equivalent to approximately 4.0 wt% MgO, about 40 times greater than the Fe-berthierine described in this study. The lowest previously reported value, from the Kursk berthierine (Klekl 1979), is 10 times greater than our Fe-berthierine. 2) The Si:Al molar ratio is lower than for most other reported berthierines (Table 2). This low silica content requires considerable Al substitution in the tetrahedral layer. Similar relationships are found for the berthierines from the Kursk area, Russia, reported by Klekl (1979) and Yershova et al. (1976), and documented in Brindley (1982). Both the Minnesota and Kursk berthierines are associated with intensive bauxitization and laterization, which is reflected in the high Al content. 3) There is little-to-no site vacancy due, perhaps, to the large-grained nature of the sample which facilitated probing of a pure sample. Parenthetically, if there is a ferric component, then octahedral vacancies could exist. The high Fe content of our reported Fe-berthierine is apparent, with molar concentrations of 2.084 and 2.126 for octahedral Fe compared to most other previously reported berthierines having values less than 2.000. Comparison of this Fe-berthierine with previously published compositions shows that these samples, along with some of the Kursk samples, approach the idealized Fe-berthierine composition (Figure 11). Other analyses listed in Brindley's (1982) paper are more siliceous and more Mg-rich, trending towards a trioctahedral composition rather than a di-, trioctahedral composition for the Fe-berthierine. The more siliceous samples represent ones forming coatings of grains from the mouth of the Amazon (Rude and Aller 1989) and Niger deltas (Porrenga 1966), or from slightly metamorphosed ones from the Japanese coal measures (Iijama and Matsumoto 1982).

Stable isotopes of siderite and recent freshwater limestones (Table 3) were used to determine whether they formed under marine or nonmarine environments. Stable isotope values of ^{13}C from siderite associated with berthierine and non-berthierine-bearing pisolitic horizons are within the range of values reported by Weber et al. (1964) in their study of freshwater siderites, and slightly enriched relative to Gehring's (1990) study of siderites from the ferriferous phases of the Northampton ironstones (Figure 12). As a further check to confirm a freshwater origin of the siderites, values from modern tufa deposits collected 20 km west of Purgatory Creek fall extremely close to Keith and Weber's (1964) average for nonmarine limestones. The ^{18}O values of siderite are more depleted than Gehring's (1990) results, but are reasonably close to those of the freshwater limestone. Thus, in addition to the abundant plant remains, stable isotopic results from siderites also indicate that the depositional environment was nonmarine. In addition, a freshwater fossil (*Unio* sp. undet) was collected from an outcrop

Table 2. Structural formulae based on 7 oxygens of berthierines from published data. Numbers 1–14 were published in Brindley (1982) and 15–21 were found in James (1966). Analyses 22–48 were analyzed by (and published in) the corresponding reference number listed in Table 1.

Number	Si	Al(tet)	Al(oct)	Fe^{III}	Fe^{II}	Mg^{II}	Mn^{II}	Vacancy
1	1.146	0.854	0.961	0.223	1.485	0.165	0.000	0.166
2	1.097	0.903	0.919	0.186	1.661	0.133	0.000	0.101
3	1.274	0.726	1.025	0.161	1.501	0.081	0.000	0.232
4	1.224	0.776	0.936	0.011	1.790	0.174	0.002	0.087
5	1.276	0.724	0.818	0.152	1.334	0.572	0.000	0.124
6	1.207	0.793	0.787	0.216	1.644	0.247	0.000	0.106
7	1.287	0.713	0.897	0.021	1.805	0.172	0.002	0.103
8	1.427	0.573	0.848	0.271	1.480	0.128	0.002	0.271
9	1.325	0.675	0.841	0.010	1.836	0.226	0.000	0.087
10	1.335	0.665	0.737	0.180	1.693	0.265	0.000	0.125
11	1.357	0.643	0.730	0.234	1.660	0.215	0.000	0.161
12	1.457	0.543	0.631	0.000	1.667	0.658	0.000	0.044
13	1.535	0.465	0.592	0.000	1.792	0.503	0.051	0.062
14	1.517	0.483	0.365	0.233	1.808	0.533	0.002	0.059
15	1.637	0.363	0.741	0.150	1.706	0.137	0.001	0.265
16	1.308	0.692	0.287	0.524	1.829	0.299	0.001	0.060
17	1.496	0.504	0.561	0.282	1.610	0.377	0.000	0.170
18	1.284	0.716	0.698	0.666	1.089	0.172	0.050	0.325
19	1.525	0.475	0.566	0.284	1.602	0.342	0.018	0.188
20	1.431	0.569	0.846	0.310	1.675	0.396	0.019	0.000
21	1.683	0.317	0.305	1.503	0.000	0.371	0.038	0.783
22	1.442	0.558	0.859	0.628	0.945	0.104	0.000	0.464
23	2.378	0.000	0.809	0.688	0.000	0.566	0.000	0.477
24	2.176	0.000	0.901	0.819	0.000	0.331	0.000	0.948
25	1.650	0.350	0.592	1.319	0.000	0.307	0.000	0.782
26	1.399	0.601	0.510	0.320	1.503	0.391	0.161	0.115
27	1.706	0.294	0.880	1.150	0.000	0.079	0.022	0.869
28	1.440	0.560	0.882	0.000	1.773	0.184	0.000	0.161
29	1.459	0.541	0.921	0.000	1.691	0.199	0.000	0.189
30	1.364	0.636	0.858	0.000	1.674	0.356	0.000	0.112
31	1.449	0.551	0.912	0.000	1.696	0.212	0.000	0.180
32	1.301	0.699	0.860	0.000	1.910	0.150	0.000	0.080
33	1.330	0.670	0.840	0.000	1.916	0.159	0.000	0.085
34	1.300	0.700	0.776	0.000	2.077	0.109	0.000	0.038
35	1.536	0.464	0.865	0.000	1.512	0.423	0.000	0.200
36	1.560	0.440	0.880	0.000	1.630	0.200	0.000	0.290
37	1.570	0.430	1.040	0.000	1.390	0.180	0.000	0.390
38	1.700	0.300	0.870	0.000	1.550	0.270	0.000	0.310
39	1.590	0.410	0.750	0.000	1.780	0.290	0.000	0.180
40	1.470	0.530	0.480	0.000	2.170	0.250	0.000	0.100
41	1.470	0.530	0.810	0.000	1.820	0.230	0.000	0.140
42	1.460	0.540	0.650	0.000	2.030	0.310	0.000	0.010
43	1.420	0.580	0.890	0.000	1.640	0.330	0.000	0.140
44	1.420	0.580	0.560	0.000	2.010	0.410	0.000	0.020
45	1.410	0.590	0.670	0.000	1.670	0.610	0.000	0.050
46	1.380	0.620	0.700	0.000	2.150	0.120	0.000	0.030
47	1.350	0.650	0.720	0.000	1.660	0.550	0.000	0.070
48	1.320	0.680	0.590	0.000	1.760	0.500	0.000	0.150
49	1.116	0.884	0.899	0.000	2.084	0.007	0.000	0.010
50	1.080	0.920	0.886	0.000	2.126	0.006	0.000	−0.018

of lignitic mud 10 km southeast of the Purgatory Creek location.

DISCUSSION

There are several dozen occurrences of berthierine described in the literature. But the unique feature of the Minnesota berthierines is not their Fe-rich chemistry, nor their large grain size, but their formation in an exclusive nonmarine depositional environment *and* their low Mg content. Another important feature is the occurrence of this Fe-berthierine in a lateritic horizon. This laterite is a nonmarine equivalent of a marine ironstone, thus forming an important sequence boundary in rocks or deposits commonly lacking important biostratigraphic horizons. These Fe-berthierines were not transported; rather, they formed *in situ* as part of a laterite weathering profile developed on a broad, low relief peneplain. The practical absence of Mg, along

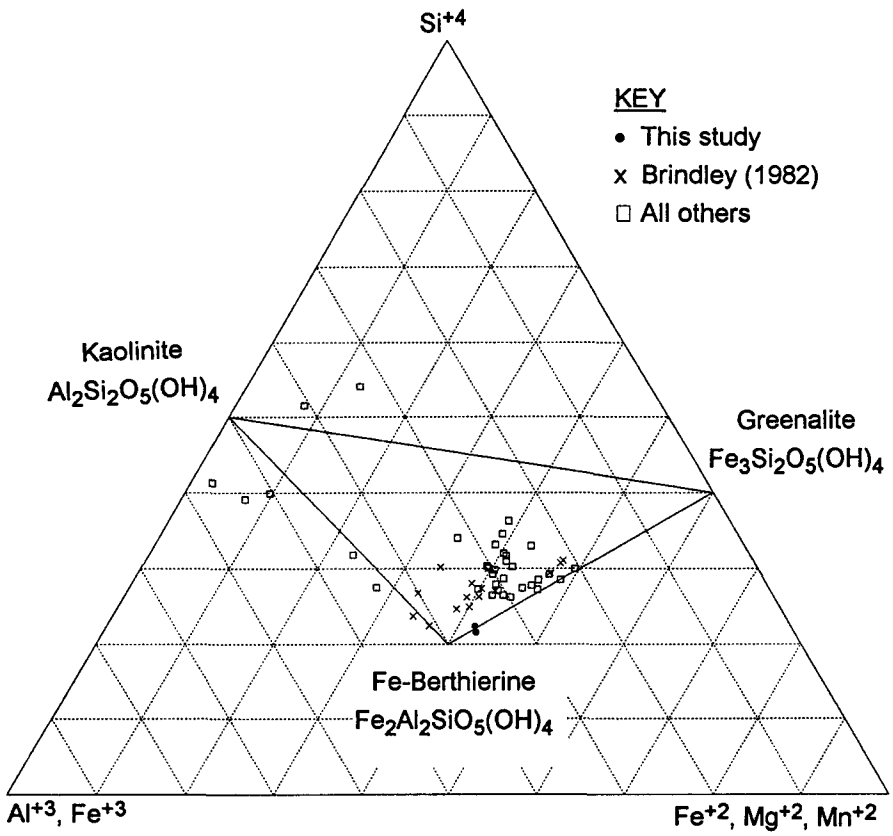

Figure 11. Plot of compositions of reported berthierines from Table 2. Open squares from samples plotting towards the kaolinite composition are from samples of modern berthierine from the Amazon and Niger deltas, which may contain impurities.

with lignite, woody concretions, occurrence with a nonmarine (unioid-like) fossil and stable isotope results support the formation of this Fe-berthierine in a nonmarine setting. During the intense chemical weathering that produced the deep saprolite, Mg and other alkaline elements were leached from the parent material, leaving only those resistate minerals containing Fe, Al, silica and titanium. Further evidence of lateritic weathering is the removal of silica from quartz and kaolinite, followed by silica-rich concretions that formed molds and casts of woody plant material. No Mg-bearing species were available from the host grains, and Mg from marine waters never came in contact with the groundwater responsible for Fe-berthierine formation.

Several workers proposed that the source of Fe for berthierine formation in marine and marginal marine settings is from detrital pisoids and microconcretions, derived from a laterite, that were reworked, transported, winnowed and deposited by sedimentary processes. Examples include reworked ooids with an outer tangential berthierine fabric (Bhattacharyya 1983), and alternating layers of either berthierine and hematite (Bhattacharyya 1989), or berthierine and carbonates

Table 3. Results of stable isotope analyses of $\delta^{13}C$ and $\delta^{18}O$ for siderite and calcite collected from berthierine and non-berthierine bearing sediments.

Sample	Description	$\delta^{13}C$	$\delta^{18}O$
OM	Ochs Mine, Morton, MN—from pisolitic horizon with no berthierine present	−2.72	−6.75
DWS	Dahlberg Mine, Redwood Falls, MN—saucer-shaped crystals formed in weathered bedrock	−5.77	−5.56
PC	Purgatory Creek—hand-picked samples from berthierine-bearing horizon	−6.17	−10.77
RR1	Renville Rhizomorph 1—tufa deposits encrusting plant roots and stems from spring in glacial drift (calcite)	−4.80	−8.29
RR2	Renville Rhizomorph 2—tufa deposits encrusting plant roots and stems from spring in glacial drift (calcite)	−4.53	−7.73

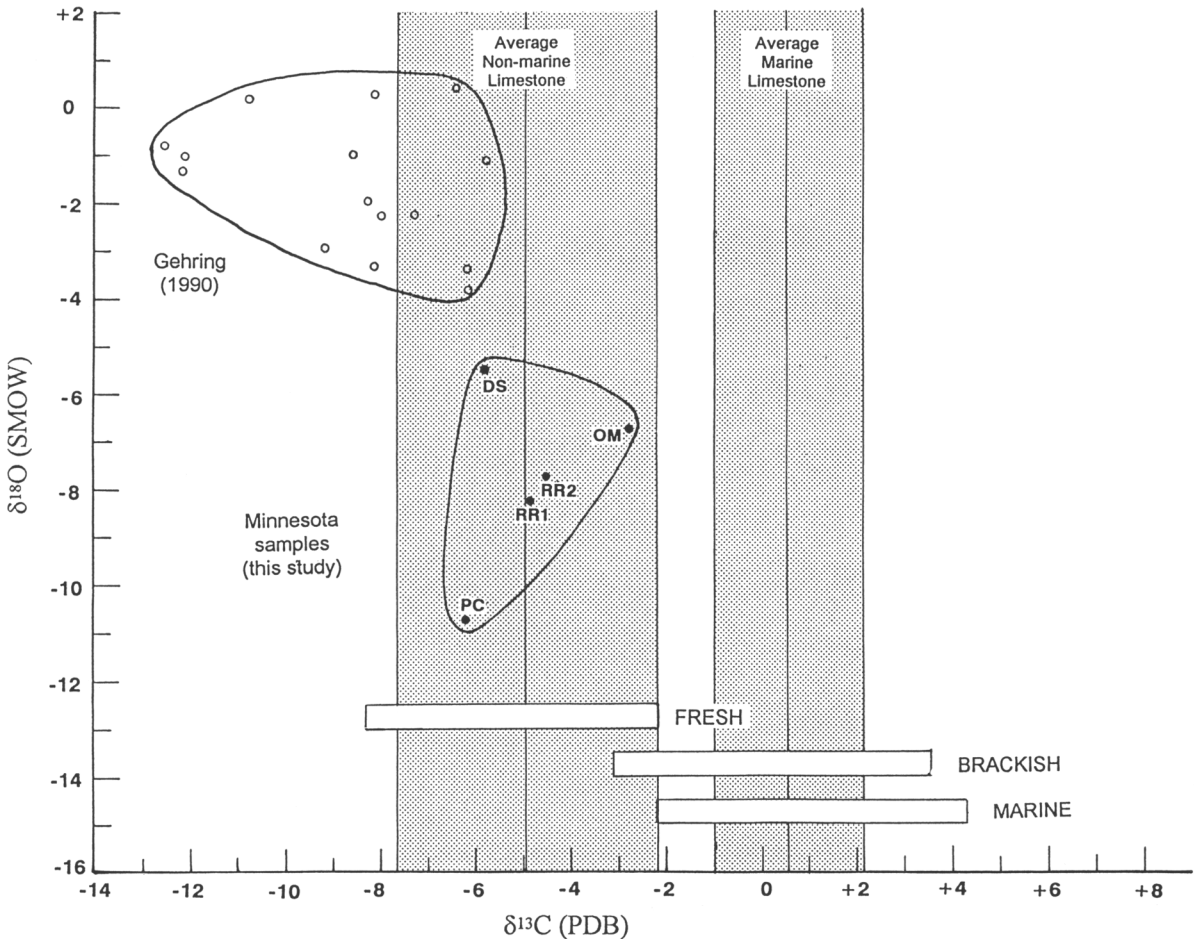

Figure 12. Plot of $\delta^{18}O$ values from siderite collected from Fe-berthierine and non-berthierine-bearing horizons as well as calcite from modern tufa deposits (See Table 3 for sample descriptions). Gehring's (1990) values are from freshwater siderites from the Northampton ironstones. Range bars at the bottom are from siderites collected from fresh-, brackish-, and marine rocks based on fossil evidence (Weber et al. 1964). Shaded areas show the ranges of $\delta^{13}C$ of nonmarine and marine limestones, with the central line representing the average (Keith and Weber 1964).

(Bayer 1989). After burial, these Fe-bearing sediments were subjected to reducing conditions leading to berthierine formation. Yet, they all formed below the sediment–water contact, with the marine waters providing Mg that was incorporated into the octahedral sites along with Fe(II). Thus, the Minnesota laterite could actually represent, by analogy, the source rocks that are commonly ascribed to Minette-type ironstones (Siehl and Thein 1989).

Stages of Early Fe-Berthierine Formation

The early stage of Fe-berthierine formation yields radial bladed and blocky grain coatings and alteration of kaolinite along grain–edge boundaries. Morphologies found with the Fe-berthierines provide evidence of formation by precipitation from solution in both unsaturated and saturated conditions. The earlier-forming Fe-berthierine formed in the vadose zone. Immediately after filling of incised channels with increasingly finer-grained sediments, alternating wet and dry periods resulted in fluctuating ground water tables as suggested by Meyer (1976) for Wealden deposits of the Paris Basin. Pisoids with desiccation, or synaeresis, cracks support such a wet-dry cycle. During wet periods and associated high water tables, organic oxidation (and the accompanying reduction of ferric Fe from goethite after complete consumption of dissolved oxygen; Curtis 1995), resulted in a solution containing ferrous Fe. Dissolved silica and alumina derived from leaching of kaolinite under lateritic conditions mixed with the ferrous Fe to form a solution saturated with respect to Fe-berthierine.

As long as the porewater was saturated with respect to Fe-berthierine, it would precipitate. Many factors affect the chemical evolution of the water prior to Fe-berthierine precipitation. If free silica (from quartz or

Table 4. Average chemistry along a transect normal to the contact between Fe-berthierine and kaolinite. Elevated values for MgO and CaO reflect contamination from epoxy mounting. Note absence of P_2O_5 in kaolinite relative to Fe-berthierine. Kaolinite is the porcelaneous cement form, Fe-berthierines the macroscopic cement.

Fe-berthierine			Kaolinite		
Oxide	Wt%	Std. dev.	Oxide	Wt%	Std. dev.
SiO_2	22.31	1.57	SiO_2	49.33	0.44
ZrO_2	0.04	0.03	ZrO_2	0.01	0.02
Al_2O_3	24.55	0.60	Al_2O_3	41.32	0.22
TiO_2	0.94	0.26	TiO_2	0.00	0.00
FeO	37.23	1.08	FeO	1.16	0.13
MnO	0.01	0.01	MnO	0.01	0.01
MgO	0.30	0.08	MgO	0.15	0.01
CaO	0.35	0.16	CaO	0.24	0.02
BaO	0.01	0.02	BaO	0.02	0.02
Na_2O	0.00	0.01	Na_2O	0.14	0.01
K_2O	0.00	0.01	K_2O	0.02	0.01
P_2O_5	0.23	0.05	P_2O_5	0.00	0.00

dissolved kaolinite) is present, H_4SiO_4 activity is too high for berthierine and gibbsite formation. If silica's activity is low but there is insufficient organic matter, then gibbsite, kaolinite and goethite are favored over the presence of minerals like siderite and Fe-berthierine that have the Fe(II) ion as an essential component. As silica concentration increases, supersaturation with respect to kaolinite occurs and excess silica is leached. Evidence of silica leaching is found in the pisolitic, but non-berthierine-bearing, horizon from an open pit kaolin mine located 10 km west of the Purgatory Creek exposure. There, where kaolinite and gibbsite were in equilibrium, siliceous concretions forming molds and casts of woody tissue, some with preserved lignite, formed localized sinks for dissolved silica.

Without adequate supplies of organic material, limited amounts of ferrous Fe are available for siderite or Fe-berthierine formation. Thus, oxidation of only the limited, scattered organic woody remains, which are preserved as lignite fragments in the argillaceous zone, led to localized Fe-berthierine formation in the form of blocky radial crystallites. Also, the fluctuating water table produced alternating periods of oxidizing and reducing conditions, causing development of gleyed soil and associated mottles. This mottling resulted in overprinting of earlier-formed pisoids by a later pisolitic texture, exemplified by the presence of larger pisoids containing smaller pisoids, with no evidence of reworking.

Stages of Late Fe-Berthierine Formation

Late stages of Fe-berthierine formation gives rise to the large, pore-filling cement, which formed during saturated groundwater conditions. As transgression of the Western Interior Seaway caused a lowering of stream gradients, streams began meandering and the development of back swamps led to deposition of organic-rich sediment that would eventually form lignite or lignitic shale. Associated with the transgression was a raised water table. This resulted in subaqueous dissolution of minerals dominated by oxidation-reduction reactions between organic matter and Fe-bearing minerals. Downward percolation of organic-rich waters derived from the swamps created conditions favorable for prolonged precipitation of berthierine as the large, pore-filling cement. The available space for Fe-berthierine's precipitation was provided by the dissolution of kaolinite and goethite, and also from infilling of partial or unfilled desiccation cracks that formed during the prior period of alternating wet and dry periods.

These diagenetic waters were oxygen-depleted and dominated by Fe reduction (Froelich et al. 1979). No sulfates were preserved in the laterite and the absence of sulfate-bearing waters produced negligible sulfide activity with the onset of reducing conditions. These suboxic, diagenetic waters resulted in Fe-berthierine precipitation through destabilization of detrital clay minerals. These Minnesota berthierines record both activities: precipitation of pore-filling Fe-berthierine cement and alteration of detrital kaolinite to berthierine (Figure 9). Taylor and Curtis (1995) describe the change in mineral stability from berthierine to siderite occurring as Fe is continually reduced with subsequent berthierine formation, which increases the pore water bicarbonate contents. Bladed siderite within an authigenic kaolinite matrix supports their observation that berthierine formation occurs during early diagenesis.

The geochemical data from a microprobe transect across the Fe-berthierine–kaolinite boundary provide evidence of the starting materials for these 2 diagenetically formed minerals (Table 4). McLaughlin et al. (1981) studied the sorption of inorganic phosphate by Fe- and Al-containing components. They showed that allophane sorbed approximately 100 times more phosphate (P) than that sorbed by gibbsite or kaolinite, with only a 10-fold difference when compared with Fe gel and its crystalline analogs, hematite, goethite and akaganeite. The amount sorbed by Fe-coated kaolinite was significantly greater than ground or dispersed kaolinite. Thus, lower P content associated with the kaolinite indicates that the kaolinite is the result of dissolution and recrystallization of a pure kaolin, precluding formation of an allophanic intermediate phase. The higher P content in the Fe-berthierine indicates that it formed as the result of dissolution of either a mixture of Fe-stained kaolinite and goethite, or from the concomitant dissolution, and later precipitation, of goethite and kaolinite, with an intermediate Fe-gel. Thus, the presence of an Fe-coated kaolinite and subsequent recrystallization would result in formation of either Fe-berthierine or a kaolinite with substantial sorbed P with associated Fe impurities. As the analyzed kaolinite contains some Fe impurities without sorbed P, its precursor was likely a mixture of kaolinite and goethite.

CONCLUSIONS

The berthierine from Minnesota, besides providing the first recorded occurrence of an Fe-berthierine, also provides the first recorded occurrence of this mineral as a macroscopic pore-filling cement formed in an exclusively nonmarine depositional environment. Other pore-filling berthierine cements from nonmarine rocks have been described (Taylor 1990; Lu et al. 1994), but their chemistry and stratigraphic relationship with overlying rocks indicate later diagenesis or marine water influence. Forming as both grain-coating and pore-filling habits indicate that it can form in both unsaturated and saturated ground water conditions.

Alteration of detrital clay minerals and reduction of ferric minerals in the absence of dissolved oxygen is necessary for Fe-berthierine formation. In the Minnesota laterite, kaolinite provides dissolved silica and Al, and goethite supplies the Fe which is reduced by oxidation of organic matter to yield Fe^{2+} essential for berthierine and siderite.

Just as Hallam and Bradshaw (1979) and Van Houten and Purucker (1984) have recognized the importance of ironstones as indicators of low detrital input and their relationship with condensed sections for marine deposits, the occurrence of berthierine or siderite in nonmarine deposits indicates a time of burial without the early diagenetic influence of marine waters and forms a sequence or parasequence boundary. Nonmarine deposits with horizons containing these ferrous-rich minerals but lacking pisolitic horizons or biostratigraphic data should be investigated by stratigraphers as a method of extending correlation of sequence boundaries with the better-documented sequence boundaries from marine deposits.

ACKNOWLEDGMENTS

We wish to thank the Clay Minerals Society for providing the senior author with a student grant to partially fund this study. Also providing support was the Indiana Mining and Mineral Resources Research Institute. S. Guggenheim of University of Illinois–Chicago gave valuable assistance with his single-crystal work of submitted berthierine samples. C. Harvey and J. Hemzacek of Indiana University aided with XRD traces. J. Lovell and C. Hager of Purdue assisted with SEM and microprobe work, respectively. J. Heine of the Natural Resources Research Institute of Minnesota helped with field collection of samples. A. Thomas (Texaco) and M. Lee (Mobil) provided helpful discussion.

REFERENCES

Bailey SW. 1988. Structures and compositions of other trioctahedral 1:1 phyllosilicates. In: Bailey SW, editor. Hydrous phyllosilicates (exclusive of micas). Rev Mineral 19:169–188.

Bayer U. 1989. Stratigraphic and environmental patterns of ironstone deposits. In: Young TP, Taylor WEG, editors. Phanerozoic ironstones. London: Geol Soc Spec Publ 46. p 105–117.

Bhattacharyya DP. 1983. Origin of berthierine in ironstones. Clays Clay Miner 31:173–182.

Bhattacharyya DP. 1989. Concentrated and lean oolites: Examples from the Nubia Formation at Aswan, Egypt, and the significance of the oolitic types in ironstone genesis. In: Young TP, Taylor WEG, editors. Phanerozoic Ironstones. London: Geol Soc Spec Publ 46. p 93–104.

Bolin EJ. 1956. Upper Cretaceous *Foraminifera, Ostracoda,* and *Radiolaria* from Minnesota. J Paleo 30:278–298.

Brindley GW. 1951. The crystal structure of some chamosite minerals. Mineral Mag 29:502–505.

Brindley GW, Youell RF. 1953. Ferrous chamosite and ferric chamosite. Mineral Mag 30:57–70.

Brindley GW. 1982. Chemical compositions of berthierines—A review. Clays Clay Miner 30:153–155.

Curtis CD. 1995. Post-depositional evolution of mudstones. 1: Early days and parental influences. J Geol Soc London 152:577–586.

Deudon M. 1955. La chamosite orthorhombique du minerai de Sainte-Barbe, couche grise. Soc Granc Miner, B 78:475–480.

Deverin L. 1945. Etude petrographique des mineris de fer oolithiques du dogger des Alpes suisses. Beitraege zur Geologie der Schweiz, Geotech. Ser, Lf 13. p 115.

Engelhardt W. 1942. Die Strukturen von Thuringit, Bavalit und Chamosit und ihre Steelung in der Chloritgruppe. Z Krist:142–159.

Floran RJ, Papike JJ. 1975. Petrology of the low-grade rocks of the Gunflint Iron-Formation, Ontario-Minnesota. GSA Bull 86:1169–1190.

Fritz SJ, Popp RK. 1985. A single-dissolution technique for determining FeO and Fe_2O_3 in rock and mineral samples. Am Mineral 70:961–968.

Froelich PN, Klinkhammer GP, Bender ML, Luedtke NA, Heath GR, Cullen D, Dauphin P. 1979. Early oxidation of organic matter in pelagic sediments of the eastern equatorial Atlantic: suboxic diagenesis. Geochim Cosmochim Acta 43:1075–1090.

Gehring AU. 1990. Diagenesis of ferriferous phases in the Northampton ironstone in the Cowthick quarry near Corby (England). Geol Mag 127:169–176.

Goldich SS. 1938. A study in rock-weathering. J Geol 46: 17–58.

Halbach P. 1970. Mineral constituents and facies development of the principal seam horizon of the Franconian Dogger beta in the area of the claim of the "Kleiner Johannes" company near Pegnitz, Upper Franconia. Geol Jahrbuch 88: 471–507.

Hallam A, Bradshaw MJ. 1979. Bituminous shales and oolitic ironstones as indicators of transgressions and regressions. J Geol Soc London 136:157–164.

Harder H. 1989. Mineral genesis in ironstones: A model based upon laboratory experiments and petrographic observations. In: Young TP, Taylor WEG, editors. Phanerozoic ironstones. London: Geol Soc Spec Publ 46. p 9–18.

Hallimond AF. 1939. On the relation of chamosite and daphnite to chlorite group. Mineral Mag 25:441–465.

Hughes CR. 1989. The application of analytical transmission electron microscopy to the study of oolitic ironstones: A preliminary study. In: Young TP, Taylor WEG, editors. Phanerozoic ironstones. London: Geol Soc Spec Publ 46. p 121–132.

Iijima A, Matsumoto R. 1982. Berthierine and chamosite in coal measures of Japan. Clays Clay Miner 30:264–274.

James HJ. 1966. Chemistry of the iron-rich sedimentary rocks. US Geol Surv Prof Paper 440-W. 59 p.

Kearsley AT. 1989. Iron-rich ooids, their mineralogy and microfabric: Clues to their origin and evolution. In: Young TP, Taylor WEG, editors. Phanerozoic ironstones. London: Geol Soc Spec Publ 46. p 141–164.

Keith ML, Weber JN. 1964. Isotopic composition and environmental classification of selected limestones and fossils. Geochim Cosmochim Acta 28:1787–1816.

Klekl LV. 1979. Regularities of chamosite distribution in bauxites of the Belgorod Distric of the Kursk magnetic anomaly. Lithol Miner Resour 14:377–382 [English translation].

Kodama H, Foscolos AE. 1981. Occurrence of berthierine in Canadian Arctic desert soils. Can Mineral 19:279–283.

Lu G, McCabe C, Henry DJ, Schedl A. 1994. Origin of hematite carrying a Late Paleozoic remagnetization in a quartz sandstone bed from the Silurina Rose Hill Formation, Virginia, USA. Earth Planet Sci Lett 126:235–246.

Maynard JB. 1986. Geochemistry of oolitic iron ores, an electron microprobe study. Econ Geol 81:1473–1483.

McLaughlin JR, Ryden JC, Syers JK. 1981. Sorption of inorganic phosphate by iron- and aluminium-containing components. J Soil Sci 32:365–377.

Meyer R. 1976. Continental sedimentation, soil genesis, and marine transgression in the basal beds of the Cretaceous in the east of the Paris Basin. Sedimentology 23:235–253.

Nikitina AP, Zvyagin BB. 1972. Origin and crystal structure features of clay minerals from the lateritic bauxites in the European part of the U.S.S.R. In: Serratosa JM, editor. Proc Int Clay Conf; Madrid. Madrid: Div Ciencias, CSIC. p 227–233.

Novak F, Losert J, Valcha Z, Vtelensky J. 1957. Orthochamosit z rudnich zil v Kanku u Kutne Hory, novy specificky mineral. Ustav Geol: 315–342.

Parham WE. 1970. Clay mineralogy and geology of Minnesota's kaolin clays. MN Geol Surv Spec Publ 10. 142 p.

Porrenga DH. 1966. Clay minerals in recent sediments of the Niger Delta. In: Bailey SW, editor. Clays Clay Miner, Proc 14th Natl Conf; 1965; Berkeley, CA. New York: Pergamon Pr. p 221–233.

Porrenga DH. 1967. Glauconoite and chamosite as depth indicators in the marine environment. Mar Geol 5:495–501.

Protic M. 1955. Etude mineralogique des phyllites de quelques minerais de fer Serbie (Yougoslavie). Soc Franc Miner, B 78:528–534.

Rohrlich V, Price NB, Calvert SE. 1969. Chamosite in the recent sediments of Loch Etive, Scotland. J Sed Petrol 39: 624–631.

Rude PD, Aller RC. 1989. Early diagnetic alteration of lateritic particle coatings in Amazon continental shelf sediment. J Sed Petrol 59:704–716.

Schellmann W. 1966. Secondary formation of chamosite from goethite. Z Erz Metall 19:302–305.

Setterholm DR. 1994. The Cretaceous rocks of southwestern Minnesota: Reconstructions of a marine and nonmarine transition along the eastern margin of the Western Interior Seaway. In: Shurr GW, Ludvigson GA, Hammond RH, editors. Perspectives on the eastern margin of the Cretaceous Western Interior Basin. Boulder, CO: Geol Soc Am Spec Paper 287. p 97–110.

Siehl A, Thein J. 1989. Mintette-type ironstones. In: Young TP, Taylor WEG, editors. Phanerozoic ironstones. London: Geol Soc Spec Publ 46. p 175–193.

Sloan RE. 1964. The Cretaceous system in Minnesota. MN Geol Surv Report of Investigations 5. 64 p.

Sudo T. 1943. On some low temperature hydrous silicates found in Japan. Bull Chem Soc Jpn. 18:281–329.

Taylor KG. 1990. Berthierine from the non-marine Wealden (Early Cretaceous) sediments of south-east England. Clay Miner 25:391–399.

Taylor KG, Curtis CD. 1995. Stability and facies association of early diagenetic mineral assemblages: An example from a Jurassic ironstone–mudstone succession, U.K. J Sed Res A65:358–368.

Thurrell RG, Sergeant GA, Young BR. 1970. Chamosite in Weald clay from Horsham, Sussex. Nat Env Res Council Rpt 70/7.

Toth TA. 1991. Part 1: Paleogeographical interpretation of Late Cretaceous, kaolinite-rich sediments of the Minnesota River Valley, Redwood, Renville, Brown, and Nicollet Counties, Minnesota. In: Hauck SA, Heine JJ, editors. Regional and local geologic, mineralogic, and geochemical controls of industrial clay grades in the Minnesota River Valley and the Meridian Aggregates Quarry, St. Cloud, Minnesota. Nat Resources Research Inst Technical Report NRRI/TR-91/15. p 1–93.

Toth TA. 1996. Stratigraphy, mineralogy, and geochemistry of Upper Cretaceous deposits from the Minnesota and Cottonwood River Valleys, southwestern Minnesota [Ph. D. dissertation]. West Lafayette, IN: Purdue Univ. 199 p.

Van Houten FB, Purucker ME. 1984. Glauconitic peloids and chamosite ooids, favorable factors, constraints, and problems. Earth-Sci Rev 20:211–243.

Velde B, Raoult JF, Leikine M. 1974. Metamorphosed berthierine pellets in Mid-Cretaceous rocks from north-eastern Algeria. J Sed Petrol 44:1275–1280.

Velde B. 1989. Phyllosilicate formation in berthierine peloids and iron oolites. In: Young TP, Taylor WEG, editors. Phanerozoic ironstones. London: Geol Soc Spec Publ 46. p 3–8.

Weber JN, Williams EG, Keith ML. 1964. Paleoenvironmental significance of carbon isotopic composition of siderite nodules in some shales of Pennsylvanian age. J Sed Petrol 34:814–818.

Witzke BJ, Ludvigson GA. 1994. The Dakota Formation in Iowa and the type area. In: Shurr GW, Ludvigson GA, Hammond RH, Editors. Perspectives on the Eastern Margin of the Cretaceous Western Interior Basin. GSA Spec Pap 287:43–78.

Yershova ZP, Nikitina AP, Perfil'ev YD, Babeshkin AM. 1976. Study of chamosites by gamma-resonance (Mössbauer) spectroscopy. In: Bailey SW, editor. Proc Int Clay Conf; 1975; Mexico City. Wilmette, IL: Applied Publishing. p 211–219.

(Received 5 February 1996; accepted 19 September 1996; Ms. 2733)